8. THE MEASUREMENT OF R-CURVES FOR A STRUCTURAL STEEL

by A.A. Willoughby* and P.L. Pratt,
Department of Metallurgy and Materials Science,
Imperial College, London

1. INTRODUCTION

The early stages of fibrous crack extension in a ductile material often demand an increase in the applied load, even though the uncracked ligament is decreasing. Krafft et al (1) ascribed this apparent rise in toughness to the growth of shear lips. Recent experiments have shown, however, that the measured resistance to crack extension may increase even in the absence of shear lips, under "plane strain" conditions (2, 3).

The fracture toughness of fully plastic, bend test-pieces may be measured in terms of the crack opening displacement (COD,δ), or the J-integral. COD may be calculated by means of Wells formula (4), and J by estimation formulae (5). During slow crack growth, various modifications to these formulae are in common use to measure the R-curve:-

(i) The COD, δ_o, referred to the position of the original crack tip (6, 7), calculated from

$$\delta_o = \frac{r(W-a_o) + \Delta a}{rW + (1-r)(a_o + \Delta a) + z}\left[V - f\left(\frac{a}{W}\right)\right] \qquad (1)$$

where r is the rotational factor, W is the specimen width, a_o the initial crack length, Δa the crack extension, z the height of the knife edges and V the clip gauge displacement.

(ii) The COD, δ_f, referred to the position of the final, growing crack tip (8). This is obtained by modifying (1).

(iii) Estimates of the J-integral (3, 9). In terms of the original crack length, making no allowances for crack extension,

$$J_o = \frac{2U}{B(W-a_o)} \qquad (2)$$

for three point bending, where U is the area under the load/deflection plot, and B the specimen thickness.

*Now at CEGB Regional Scientific Services, Portishead, Bristol.

2. RELATIONSHIP BETWEEN δ_o, δ_f, and J_o IN THREE POINT BENDING

a) $\delta_o + \delta_f$

Referring to Fig. 1, by similar triangles,

$$\frac{\delta_f}{r\,(W-a_o-\Delta a)} = \frac{\delta_o}{\Delta a + r(W-a_o-\Delta a)} \qquad (3)$$

The δ_o vs. Δa curve is normally linear, at least in the early stages of crack extension.

i.e. $\delta_o = A\Delta a + \delta_i$ (4)

where A is the slope and δ_i the initial COD.
Hence, from (3) and (4)

$$\delta_f = \frac{(A\Delta a + \delta_i)\, rb}{rb + \Delta a} \qquad (5)$$

where $b = W - a_o - \Delta a$. If $\delta_i \ll r\,A(W-a_o)$, the initial slope is

$$\left.\frac{d(\delta_f)}{d(\Delta a)}\right|_{\Delta a = o} = A \qquad (6)$$

Thus, the initial slopes of the δ_f & δ_o R-curves are approximately the same, for sufficiently large specimens. Equation (5) may be used to predict the whole of the δ_f rs. Δa curve. Note that δ_f is not the actual COD of the propagating crack tip (denoted by δ_p in Fig 1), but is a geometrical consequence of the mouth opening and centre of rotation of the test piece.

b) $\delta_o + J_o$

Equation (2) may be rewritten

$$J_o = \frac{2\int M\, d\theta}{B'(W-a_o)} \qquad (7)$$

where M is the bending moment and θ is the angle of bend, given approximately by

$$\theta = \frac{\delta_o}{rb + \Delta a} \qquad (8)$$

Combining with (4) and differentiating gives

$$\frac{d\,\theta}{d(\Delta a)} = \frac{Ar\ (W-a_o) - \delta_i\ (1-r)}{(rb + \Delta a)^2} \qquad (9)$$

Substituting in (7) gives

$$\frac{d\,J_o}{d(\Delta a)} = \frac{2M}{B'(W-a_o)} \quad \frac{d\,\theta}{d(\Delta a)} \qquad (10)$$

This may be integrated to give the complete J_o R-Curve. For rigid-plastic behaviour, the bending moment is given by

$$M = 0.31\sigma_y\ B'b^2$$

Some allowance for work hardening may be made by substituting $\sigma_{flow} = (\sigma_y + \sigma_{uts})/2$ in place of σ_y.

At $\Delta a = o$, (10) becomes

$$\left.\frac{dJ_o}{d(\Delta a)}\right|_{\Delta a=o} = \frac{0.62\sigma_{flow}}{(W-ao)r^2} \left\{ Ar\ (W-a_o) - \delta_i(1-r) \right\} \qquad (11)$$

which simplifies to

$$\left.\frac{dJ_o}{d(\Delta a)}\right|_{\Delta a=o} = \frac{0.62\sigma_{flow}}{r}\ A \qquad (12)$$

if $\delta_i \ll A(W-ao)$. This equation is analogous to $J=M\,\sigma_{flow}\,\delta$, which applies up to initiation. Taking r=0.45, the factor corresponding to M is 0.62/0.45 = 1.4, which is in agreement with the theoretical and experimental values for M of 1-2.5.

3. EXPERIMENTAL DETAILS

R curves were measured on a hot-rolled, low strength steel (En32B), the composition of which is given in Table 1. It contained elongated manganese

sulphide inclusions. Precracked, three point bend test-pieces were used, 10 mm. square and with a 40 mm. span. They had 2 mm. deep side-grooves to eliminate shear lips. To develop an R-curve several test pieces were required. These were loaded to different displacements to give varying amounts of slow crack growth, and then broken open at low temperature in the cleavage mode. Crack lengths were measured optically on the fracture surface at nine different points along the crack front. The clip gauge and load point displacements were monitored continuously during slow crack growth, so that δ_o and J_o could be calculated for each specimen.

Two heat treatments, normalising and slow cooling, were used, and these resulted in yield stresses of 290 and 220 MN/M^2 respectively. The effects of nominal prestrains of 10 and 20% and of test-piece orientation (as defined in Fig. 2) were also investigated.

Strains around the crack tips were estimated by two methods, microhardness and recrystallisation (10). The latter technique was used for the high strains in the immediate vicinity of the tip. Specimens were heat-treated at 650°C for 3 hours, and sectioned. The number of recrystallised grains in a small region at the crack tip could be related to the average strain there by means of a prior calibration performed on tensile specimens.

4. EXPERIMENTAL RESULTS

Some typical R-curves in terms of δ_o and J_o are shown in Figs. 3 and 4. These enabled the initial values, δ_i and J_i, and the slopes, to be measured.

a) Initiation

Both δ_i and J_i were affected by prestrain and by specimen orientation with respect to the orientation of elongated inclusions. Further discussion, however, is beyond the scope of this paper.

b) Propagation

The initial slopes of the R-curves are given in Table 2. Changes in yield stress had a negligible effect. Prestrain tended to lower the initial slopes. Test-piece orientation had a large influence. The initial slopes may be divided approximately into two categories:

LS, LT $\gg$ TS, ST, TL, SL

In the first category the elongated manganese sulphide inclusions were aligned parallel to the maximum tensile stress, normal to the crack plane. In the second category they lay in the crack plane.

Also shown in Table 2. is a comparison between the measured initial slope of the J_o R-curve, and that predicted from equation (11), using the measured values of A. Agreement is good for the less tough orientations, and where the work-hardening capacity had been lowered by prestrain. Poorer agreement is expected in cases of high work-hardening, as a result of the essentially rigid-plastic analysis.

c) The Strain at the Crack Tip.

The average true strain in a region 50 mm. square was estimated by means of the recrystallisation technique. Fig. 5. shows that this strain remained constant during crack extension, in contrast to the observed steep rise in the R-curves. The lateral extent of the plastic zone was determined by micro-hardness measurements on sectioned specimens in different orientations, all with 1 mm. of crack extension. Fig. 6 shows that this was larger in the tougher specimen (LS orientation). The difference in hardness levels remote from the crack in the TS and TL specimen reflects the fact that they had been normalised in different batches.

5. DISCUSSION

The variation of toughness with microstructure may be explained on the basis of the attainment of a critical fracture strain over a small region ahead of the crack tip. By prestraining, the additional strain required to reach this critical value is lowered and the toughness reduced. The dependence on inclusion orientation is caused by the "plastic strain intensification", F, of the inclusions. The plastic strain, ε' in the ligament between the crack tip and an inclusion may be written:

$$\varepsilon' = \varepsilon (1+F)$$

where ε is the plastic strain in the absence of the inclusion. F may be expected to increase with decreasing separation of inclusions (assuming these are weakly bonded to the matrix), and with increasing inclusion length perpendicular to the maximum tensile stress.

The analytical relationship between $dJ_o/d(\Delta a)$ and A, Eqn. (12), for rigid-plastic materials, contains no factors dependent on specimen size. Therefore, if A is geometry independent, $dJ_o/d(\Delta a)$ should be too, initially. This seems likely, for a large test-piece, since A may be identified as the angle between the growing crack flanks (3), and so should be characteristic of the crack tip (11). However, the strains at the growing crack tip were found to be constant, and previous work (12) has shown that the COD, δ_p in Fig. 1, at the propagating crack tip is invariant. This evidence, together with the observed increase in plastic zone extent with increasing toughness, implies that the rise in the R-curve is caused by an increase in remote plastic work, which is geometry dependent.

The apparent contradiction may be reconciled as follows. Just prior to initiation, unique stress and strain fields, as determined by δ or J, are set up over a region ahead of the crack tip, and these are size independent. The crack then extends into these fields. The initial spread of plasticity from the crack tip is dependent upon local conditions, which are determined by the interaction of the microstructure with the stress and strain fields. Thus the initial slope of the R-curve is dependent upon the conditions at the crack tip.

A criterion for J-controlled crack growth was proposed by Paris et al (13) as

$$\omega \gg 1$$

where $\omega = \frac{W-a}{J} \frac{dJ}{da}$

For the tougher orientations, (LS and LT) $\omega \simeq 25$ at initiation. However, for the other orientations, $\omega \simeq 5$, and decreases with crack extension. This provides a possible explanation for the greater non-linearity observed in the J_o R-curves in these orientations, since the lower values of ω would imply that the crack extension was influenced by specimen geometry.

Acknowledgements

The authors thank the Science Research Council for financial support and Prof. J.G. Ball for the provision of research facilities.

REFERENCES

1. J.M. Krafft et al. Proc. of the Crack Propagation Symposium, (1961), Cranfield, 1, p.8.

2. S.J. Garwood and C.E. Turner, Proc. of the Fourth Int. Conf. on Fracture, Waterloo (1977), 3, p.279.

3. C.F. Shih et al. ASTM Symp. on Elastic Plastic Fracture, Atlanta (1977). To appear as ASTM STP.

4. British Standard Draft for Development, DD19 (1972).

5. J.R. Rice et al. ASTM STP 536 (1973), p.231.

6. D. Elliott et al. Proc. of Conf. on the Practical Application of Fracture Mechanics to Pressure Vessel Technology (1971), London, p.217.

7. R.F. Smith and J.F. Knott, ibid, p.65.

8. K. Tanaka and J.D. Harrison. Welding Institute Report R/RB/E73/76 (1976).

9. J.A. Begley and J.D. Landes ASTM STP 560 (1974), p.170.

10. T. Shoji, Metal Science, 10, (1976) p. 165.

11. G. Green and J.F. Knott. J.Mech. Phys. Solids, 23, (1975), p.128.

12. S.T. Garwood and C.E. Turner. Submitted to Int. J. Fracture Current Research Reports (1978).

13. P.C. Paris et al ASTM Symp. on Elastic Plastic Fracture. Atlanta (1977). To appear as ASTM STP.

TABLE 1.

Chemical Composition of En 32B Steel, in weight %

C	Si	Mn	S	Ni	Cr	Mo	Cu
0.17	0.23	0.74	0.033	0.02	0.01	0.01	0.08

TABLE 2.

Initial slopes, A (= $d\delta_o/d\ (\Delta a)$ and $dJ_o/d(\Delta a)$, of the R-curves

Condition and orientation		A	Initial $dJ_o/d(\Delta a)$ MJ/m^3	
		Measured	Measured	Predicted from (11)
Normalised	LT	0.70	540	340
	LS	0.69	590	340
	TS	0.21	83	94
	ST	0.18	78	83
	TL	0.15	98	71
	SL	0.17	92	81
Slow cooled	LS	0.80	590	320
	TS	0.18	83	60
Prestrained 10%	LS	0.50	670	350
	TS	0.02	12	6
Prestrained 20%	LS	0.50	407	457
	TS	0.02	13	13

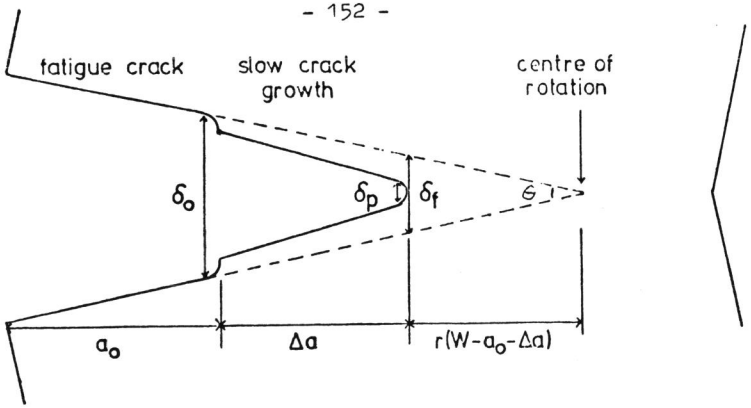

Fig.1 The geometrical relationship between different CODs in three point bend.

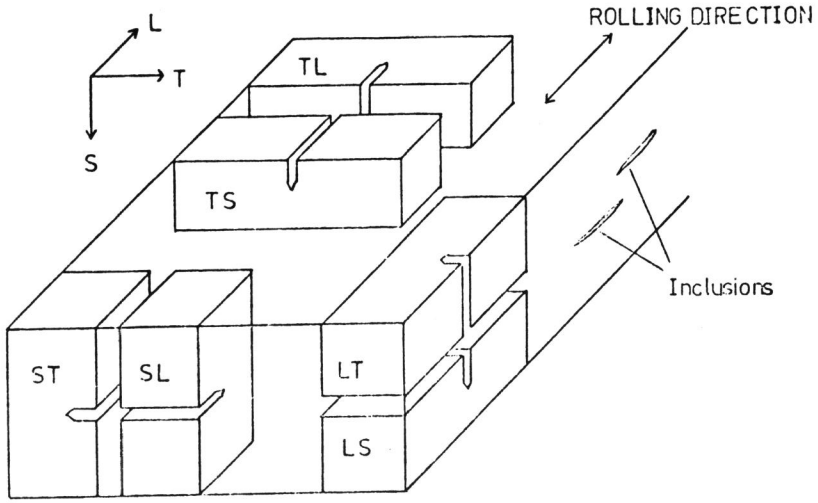

Fig.2 Orientation of test-pieces.

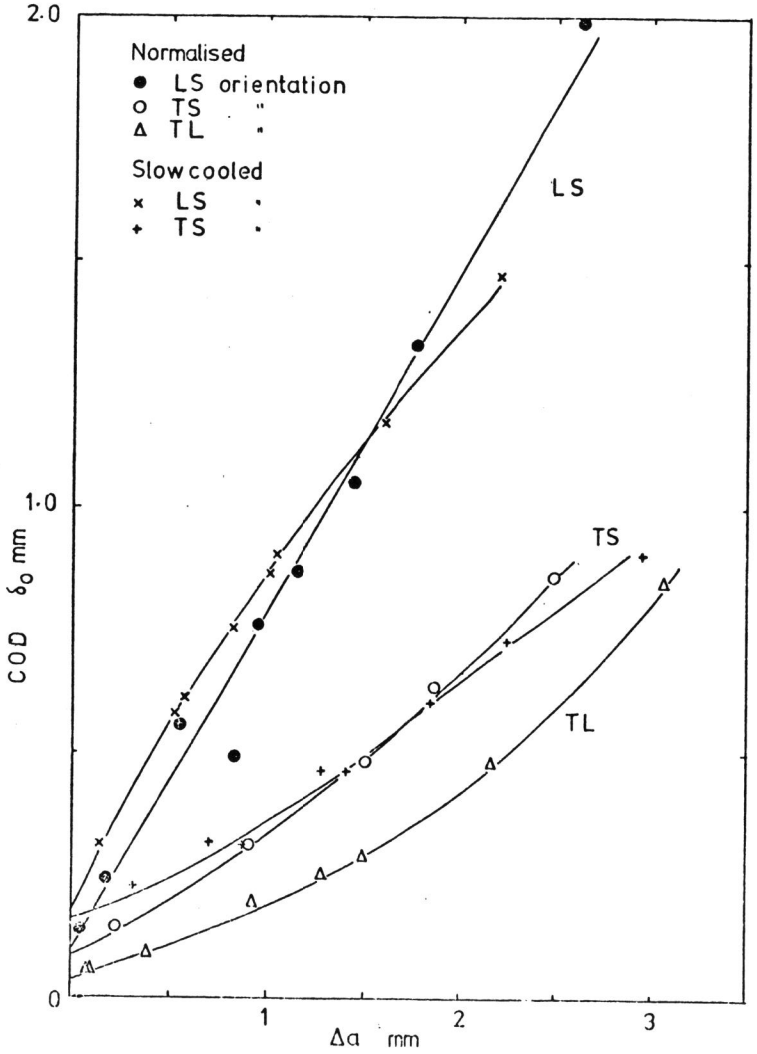

Fig.3 Effect of heat treatment and orientation on the δ_o R-curve, En32B.

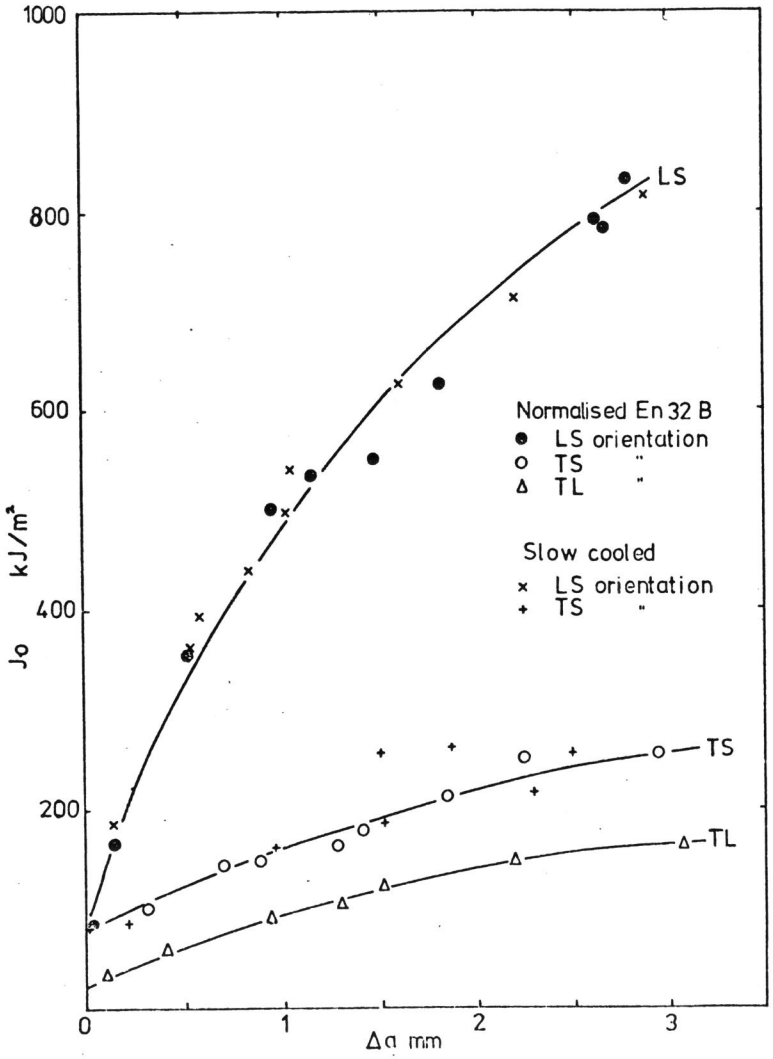

Fig.4 Effect of heat treatment and orientation on the J_0 R-curve, En32B.

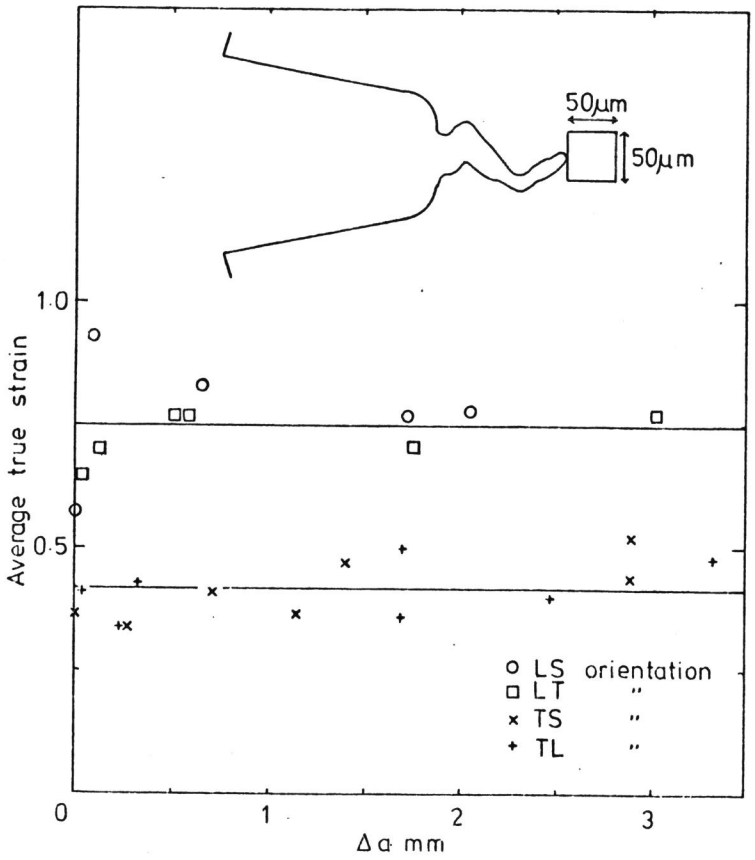

Fig.5 Variation with Δa of true strain in a region 50 μm square at the crack tip, as estimated by recrystallisation.

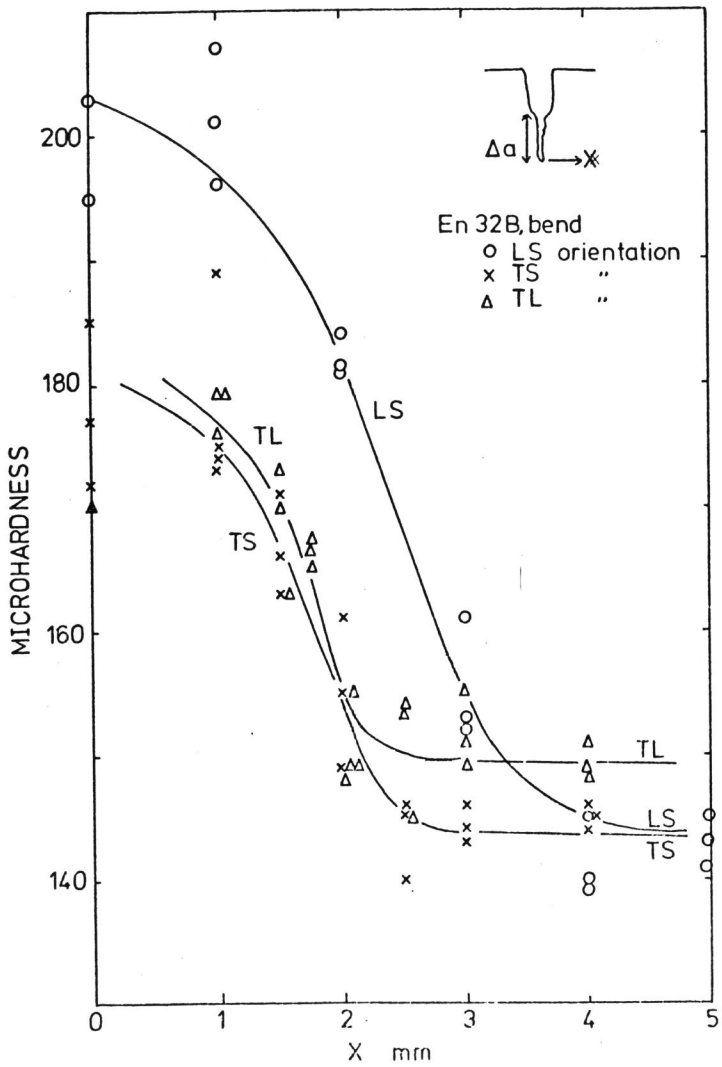

Fig.6 Microhardness profile around crack tips in En32B, showing lateral extent of the plastic zone. Δa = 1mm.